INL/JOU-22-70510-Revision-0

A short review of defect superlattice formation in metals and alloys under irradiation

February 2022

Cheng Sun

Changing the World's Energy Future

INL is a U.S. Department of Energy National Laboratory operated by Battelle Energy Alliance, LLC

INL/JOU-22-70510-Revision-0

A short review of defect superlattice formation in metals and alloys under irradiation

Cheng Sun

February 2022

Idaho National Laboratory
Idaho Falls, Idaho 83415

http://www.inl.gov

Prepared for the
U.S. Department of Energy
Under DOE Idaho Operations Office
Contract DE-AC07-05ID14517

Journal of Nuclear Materials 559 (2022) 153479

Contents lists available at ScienceDirect

Journal of Nuclear Materials

journal homepage: www.elsevier.com/locate/jnucmat

A short review of defect superlattice formation in metals and alloys under irradiation

Cheng Sun

Idaho National Laboratory, Idaho Falls, ID 83415, United States

ARTICLE INFO

Article history:
Received 12 November 2021
Revised 10 December 2021
Accepted 11 December 2021
Available online 14 December 2021

Keywords:
Irradiation
Gas bubble superlattice
Void superlattice
Metals and alloys

ABSTRACT

Irradiation damage drives complex and coupled phenomena in materials at far-from-equilibrium conditions. The self-organization of nanoscale defects in materials under irradiation shows great potential to tailor the physical properties of materials by controlling nanopatterned microstructures. Irradiation-induced gas bubble and void superlattices are two important ordered nanostructures of great scientific interest. Although both types of superlattices have been investigated extensively, a consensus has yet to be reached on their formation mechanisms. In this review article, the current research status of gas bubble and void superlattices in metals and alloys and their characterization, structural stability, and mechanistic modeling are summarized. The fundamental research goals to advance the mechanistic understanding of gas bubble and void superlattices are outlined.

1. Introduction

The self-organization of defects in materials leads to the formation of ordered defect superlattices. Self-organization has gained significant interest as an approach to create nanomaterials with tailored physical properties in which defects are used as building blocks to form ordered microstructures. For example, Jia et al. demonstrated that the self-assembly of thiolated Ag nanoclusters leads to intriguing photophysical features and multicolor emissions that can be applied in imaging, sensing, and photovoltaics [1]. The formation of ordered defect superlattices could be useful in nuclear fuels to effectively store the fission gas and prevent large structural distortions due to swelling, because ordered fission gas bubbles could prevent bubble interconnection that drives detrimental behaviors [2]. Irradiation is a versatile tool to modify the microstructure and chemistry of materials and has been successfully employed to create defect superlattices in metals, ceramics, and semiconductors. Under irradiation, energetic particles such as electrons, ions, and neutrons bombard materials and form non-equilibrium conditions, resulting in supersaturated defects such as vacancies and interstitials. The migration, annihilation, and aggregation of these defects cause complex microstructural evolution, and the ordering of defects occurs under certain irradiation conditions.

Void superlattices were first reported by Evans in early 1970s [3]. In his work, voids formed three-dimensional arrays in molybdenum (Mo) under 2 MeV nitrogen ion irradiation at 870 °C. Since then, void superlattices have been observed in many other body-centered-cubic (bcc), face-centered-cubic (fcc), and hexagonal-close-packed (hcp) metals and alloys [4–7], and electron and neutron irradiation have also produced void superlattices. Ghoniem et al. summarized the void superlattices observed in irradiated fcc and bcc metals [8]. In general, void superlattices form during a steady swelling regime over a wide range of temperatures (~0.25 to ~0.5 T_m, where T_m is the melting temperature of the host matrix), and voids are randomly distributed outside the tempeature range. The void diameter ranges from a few to a few tens of nanometers and the void lattice constant is typically a few tens of nanometers. Consistent with Evans's discovery, the void superlattice in ion irradiated fcc and bcc metals typically exhibits a crystallographic structure identical with the host matrix.

Similar to void superlattices, gas bubble superlattices (GBS) have been observed in a number of fcc, bcc, and hcp metals under irradiation. The gas can originate from either implanted gas ions or nuclear transmutation. Compared to void superlattices, the temperature required for GBS formation is relatively lower (~0.15 to ~0.3 T_m), and the bubble diameter and bubble lattice constant are both smaller. Johnson et al. reported helium (He) GBS in a variety of metals under He ion implantation, such as Mo, vanadium (V), tungsten (W), chromium (Cr), iron (Fe), and tantalum (Ta). The random He gas bubbles become He GBS at temperatures around ~0.2 T_m [9]. The ratio of gas bubble lattice constant to bubble diameter commonly falls between 2 and 5. Similar to void lattice structures, GBS typically exhibits the same crystallographic structure as the matrix.

E-mail address: Cheng.Sun@inl.gov

https://doi.org/10.1016/j.jnucmat.2021.153479

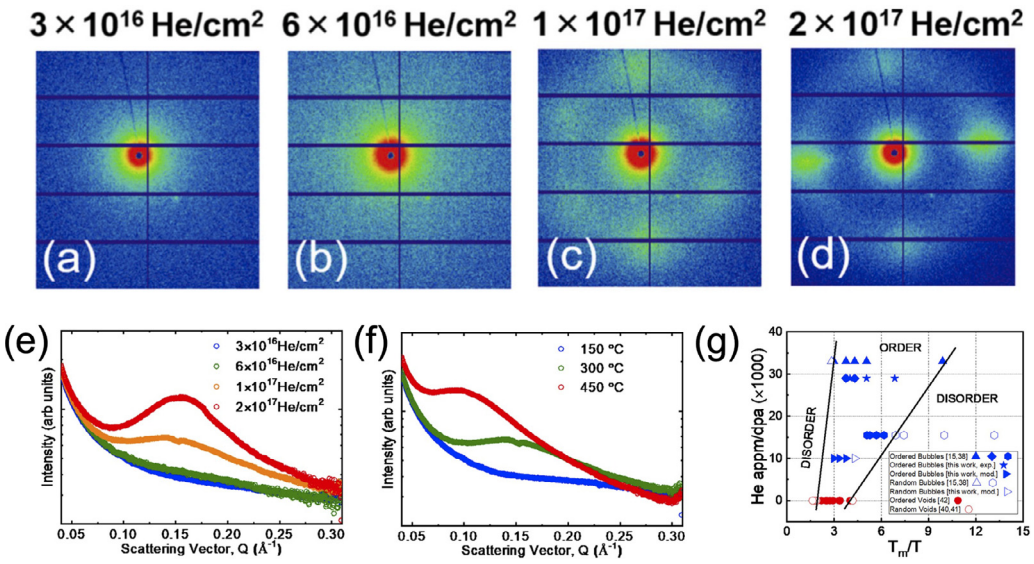

Fig. 1. Transmission small-angle X-ray scattering of He implanted Mo. (a-d) X-ray diffraction patterns of He GBS in Mo irradiated to an ion fluence from 3×10^{16} to 2×10^{17} He/cm^2 at 300 °C. (e) Plot of intensity vs scattering vector with a fluence from 3×10^{16} to 2×10^{17} He/cm^2 at 300 °C. (f) Plot of intensity vs scattering vector at temperatures from 150 to 450 °C with a fluence of 1×10^{17} He/cm^2. (g) Formation window of ordered gas bubble lattice and void lattice in Mo in terms of He appm/dpa and irradiation temperature (T_m/T). (Please see ref. [10] for the citations in the figure legend) [10].

To date, significant advance has been made in the formation, characterization, and modeling of defect superlattices in materials under irradiation. This review aims to summarize the recent research progress on the creation of defect superlattices in metals and alloys by irradiation, their advanced characterization using high-energy X-rays, the structural stability of defect superlattices in harsh environments, and their mechanistic modeling. The fundamental research needed to further advance the understanding of defect superlattice formation is also highlighted.

2. Formation of gas bubble and void superlattices

Irradiation-induced gas bubble and void superlattices have been reported in a variety of metal and alloy systems. The development of defect superlattices is strongly linked with irradiation conditions and material properties. The irradiation parameters, i.e., temperature, ion fluence, flux, and gas-atomic-parts-per-million/displacement-per-atom (appm/dpa) are critical to the formation of gas bubble and void superlattices. The temperature-, fluence-, and flux- dependent He GBS formation has been studied in bcc Mo (Fig. 1) and W [10,11]. He GBS is developed in Mo at temperatures between 150 and 450 °C; below the lower limit, He gas bubbles are randomly distributed, and above the upper limit, the ordered GBS become disordered. Increasing the ion fluence improves the ordering of He bubbles, until a GBS is formed. Once the He GBS forms, the bubble lattice constant does not change with increasing ion fluence. The higher ion flux leads to better bubble ordering, smaller bubbles size, and smaller bubble lattice constant. The effect of gas atoms is represented by the gas appm/dpa ratio. With increasing He appm/dpa ratio, the lower temperature bound for GBS formation is reduced, which could be a result of the high binding energy between He atoms and vacancies stablizing vacancies against recombination with self-interstitial atoms (SIAs). In addition, increasing the He appm/dpa ratio decreases the bubble superlattice constant, as shown in W [12]. It is also interesting to note that the irradiation conditions for void superlattices, with a He appm/dpa ratio of zero, fall within the same formation window for GBS, as seen in Fig. 1g, implying that a possible unified theory could be developed for both gas bubble and void superlattices.

Material properties, such as chemical complexity and crystal structure, have an important impact on the development of defect superlattices. The effect of the chemical complexity of the host materials on He GBS formation is studied in equiatomic concentrated solid solution alloys of FeNi and FeCrNiCo [13]. Increasing the chemical complexity (i.e., going from FeNi to FeCrNiCo) increases both the ion fluence and flux required to form He GBS. Chemically biased diffusion of SIA clusters leads to smaller bubble lattice constant and smaller bubble size. In addition, the structure of superlattices is dependent on the crystal structure of host materials. In fcc and bcc metals, gas bubble and void superlattices typically show the same cubic structure as the host materials. For example, the spatial arrangement of He gas bubbles in perforated Mo foils evolves from random bubbles to planar ordering on {110} planes, and then to three-dimensional superlattices that show the same bcc structure as Mo [10]. Unlike the cubic structure of GBS in fcc and bcc metals, superlattice in hcp metals and alloys are ordered on planes parallel to the basal planes. However, within each bubble plane, bubbles are randomly distributed. Evans et al. reported that krypton (Kr) bubbles in titanium (Ti), zirconium (Zr) and Zr alloys are spatially ordered in planes or rafts parallel to the basal planes under irradiation at temperatures from ambient up to at least 400 °C [14,15]. Consistent with the spatial arrangement of Kr bubbles in Ti and Zr, He bubbles in α-Zr also show good alignment along the basal plane after He implantation at 200 °C [16].

Although historical investigations have reported isomorphic structures of gas bubble and void superlattices to their host materials, some recent studies have reported superlattice structures that differ from host materials. Unlike the bcc structured He GBS in perforated Mo foil, He GBS in bulk Mo shows an unexpected tetragonal structure [17]. The lattice constant of He GBS measured from the in-plane orientation is larger than that measured from the out-of-plane orientation. One possible mechanism proposed for such difference is the change in elastic stress induced by bubble swelling between foil and bulk materials, however, the effect of stress on the formation of GBS needs further investigation. Another example of GBS lattice type deviation from host materials is the mixed xenon-krypton (Xe-Kr) bubbles in bcc structured γ U-Mo [18]. The Xe-Kr GBS are created in U-Mo alloys irradiated with neutrons at around 100 °C to a fission density of

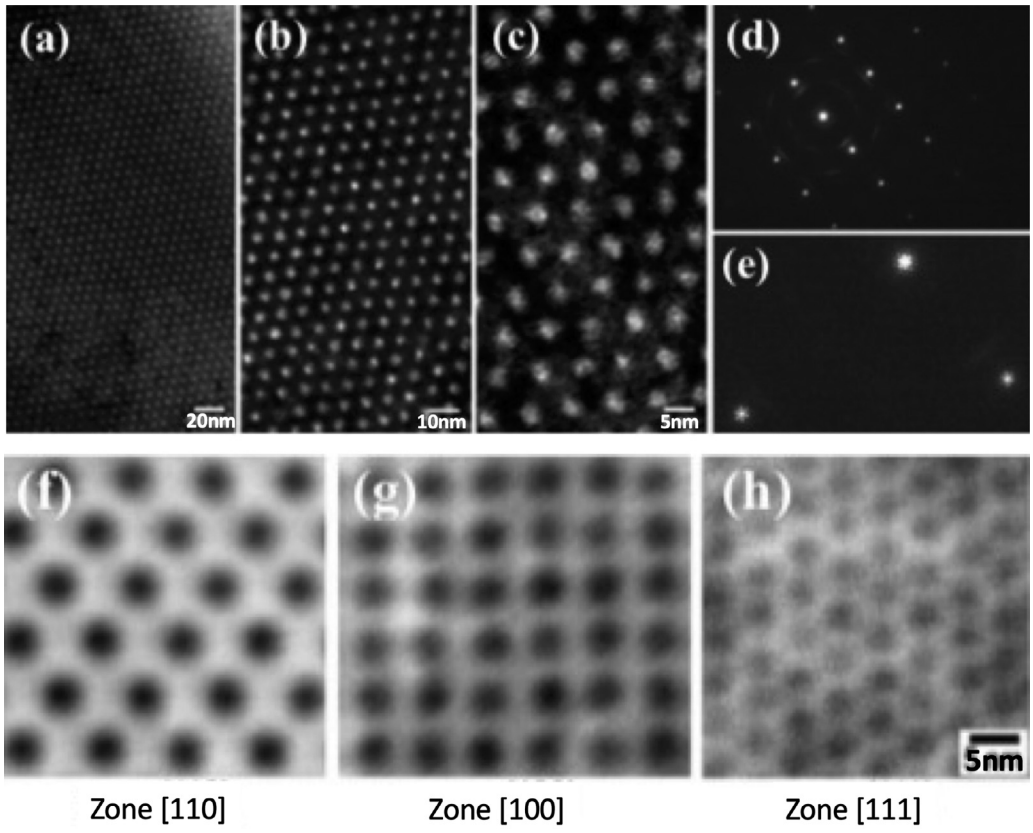

Fig. 2. (a-c) TEM micrographs of fission gas bubble superlattice in neutron irradiated U-Mo alloy at different magnifications. (d-e) Electron diffraction pattern at [011] zone axis showing an fcc structured Xe-Kr GBS in bcc U-Mo. (f-h) STEM micrographs at three different zones confirming the Xe-Kr GBS has an fcc structure. [18].

4.5 x 10^{21} fissions/cm^3. The Xe-Kr GBS show an fcc structure in bcc U-Mo that has been confirmed by transmission electron microscopy (TEM) and high-resolution scanning transmission electron microscopy (STEM), as shown in Fig. 2.

3. Characterization using synchrotron high-energy X-rays

The nanoscale defects and features in irradiated materials have been characterized by synchrotron high-energy X-ray techniques, such as X-ray powder diffraction (XRD), small-angle X-ray scattering (SAXS), X-ray absorption spectroscopy (XAS), nano-diffraction/imaging, and X-ray fluorescence (XRF). Compared to electron microscopy techniques, high-energy X-rays offer a more global measurement of nanoscale defects and defect symmetry, and the flexibility of selecting X-ray energy that allows macroscopic characterization of nanoscale structures in irradiated materials [19].

Recently, high-energy X-rays have been used to characterize defect superlattices in materials. The structure, chemical composition, and lattice strain of defect superlattices have been successfully characterized by synchrotron high-energy X-rays. Grazing incident small-angle X-ray scattering (GISAXS), a surface characterization technique, has been used to study the spatial arrangement of He gas bubbles in Mo [17]. The two-dimensional GISAXS pattern of He implanted Mo shows additional scattering spots from He gas bubbles, suggesting their spatial ordering of He gas bubbles. Both bubble size and bubble lattice constant are measured. The examination of bubble pressure is critical for determining the phase of the atoms within bubbles. X-ray absorption near edge structure (XANES) has been used to measure the atomic structure of Kr bubbles within Mo and their vibrational properties (Fig. 3) [20]. A "white-line" in the XANES spectra is observed at the Kr K-edge absorption, followed by oscillations representing the backscattering from Kr neighbors. By comparing the “white-line” peak under various pressures, the inner pressure of Kr bubbles is estimated to be ~2 GPa (Fig. 3c). Molecular dynamics simulations show that the phase of Kr atoms in the bubbles evolves from gas to liquid, and then solid as the Kr-to-vacancy ratio increases. By decreasing the temperature from 673 to 300 K, the Kr-to-vacancy ratio required for liquid-to-solid transition decreases from 0.3–0.35 to 0.15–0.25. At 2 GPa, the Kr-to-vacancy ratio of the bubbles is 0.28 at 300 K, indicating that the Kr bubbles are solid in nature. Multi-model high-energy X-ray techniques have been developed to characterize irradiated materials, allowing more comprehensive characterization. A coupled XRF and nano-diffraction/imaging technique has been used to examine defects, elemental distribution, and lattice strain in single-crystal W after Kr implantation [21]. The X-ray nano-diffraction/imaging study reveals that a complex network of local defect structures in irradiated W and a significant structural change across the irradiated and non-irradiated regions. Lattice strain measurements based on a quantitative analysis of nano-diffraction data suggest a clear increase in the lattice constant in the Kr irradiated region.

Small-angle X-ray scattering (SAXS) provides quantitative information of nanostructures in irradiated materials. SAXS has been employed to measure the evolution of gas bubble size and bubble lattice constant of He GBS in Mo and W at various fluences, temperatures, and fluxes [10,11]. Fig. 1 shows the temperature- and fluence- dependent He GBS formation in Mo, characterized by SAXS. The bubble lattice constant is insensitive to the ion fluence, but increases with increasing temperature and decreases with increasing flux. SAXS has also been used to characterize the ordering of solid bubble superlattice (Fig. 3b) [20]. The measurement of the Kr bubble size and lattice constant by SAXS agrees well with the

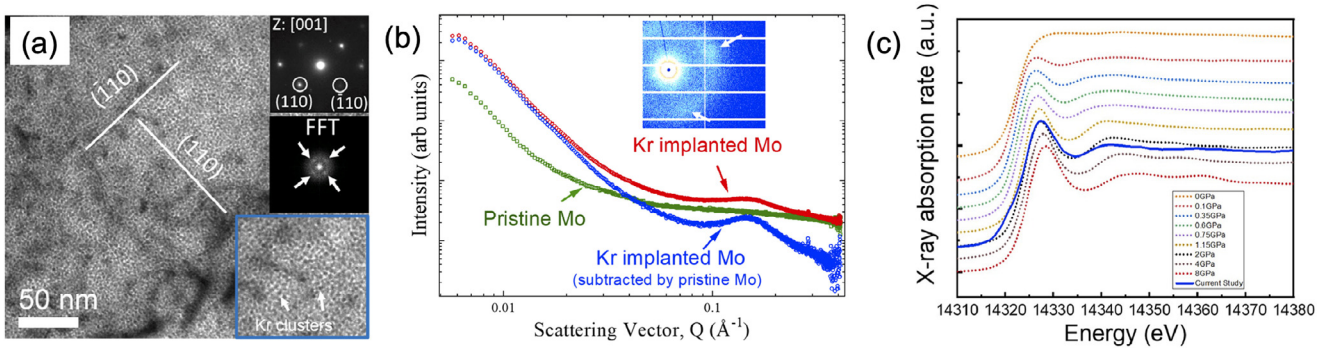

Fig. 3. Solid bubble superlattices in Kr implanted Mo. (a) TEM micrograph showing Kr bubble superlattices in Mo under Kr ion implantation at 400 °C to a fluence of $2.5 \times 10^{16}/cm^2$. (b) SAXS measurement of Kr bubble superlattices in Mo. The 2D diffraction pattern and the plot of intensity as a function of scattering vector indicate the formation of Kr bubbles superlattices. (c) XANES measurement of inner pressure of solid Kr bubbles in Mo. The inner pressure of solid Kr bubbles is ~ 2 GPa. [20].

measurement by TEM (Fig. 3a). The early-stage self-organization of Kr solid bubbles in Mo has been systematically studied by SAXS [22]. The critical fluence for the onset of Kr bubble ordering changes with implantation temperature. Similar to the He GBS, the Kr bubble lattice constant show negligible dependence on ion fluence, but increases with implantation temperature. The 2D SAXS diffraction patterns suggest that Kr solid bubbles are only weakly ordered in comparison to He GBS.

4. Structural stability in harsh environments

Studying the structural stability of defect superlattices could help uncover superlattice formation mechanisms and help design irradiation-tolerant superlattice microstructures. The structural stability of GBS and void lattices at high temperatures and under irradiation has been studied recently. The GBS with Xe-Kr bubbles in U-Mo alloys shows exceptional thermal stability. During an *in-situ* TEM heating test up to 0.78 T_m, no significant changes in bubble size or lattice constant are observed [23]. Compared to the GBS created by large noble gas atoms, He GBS created in Mo is only thermally stable up to 0.39 T_m [24]. When annealed at 0.44 T_m for one hour, the ordered He bubbles become disordered and the average bubble size increases from 1.1 to 1.6 nm [25]. The unexpected high thermal stability of gas bubbles with large noble gas atoms has been studied with integrated *ab initio* calculations and kinetic Monte Carlo simulations [26]. A unified theory for describing the energetics of He, neon (Ne), argon (Ar), and Kr bubbles in bcc metals in group 5B (V, Nb, Ta), 6B (Cr, Mo, W) and 8B (Fe) is developed and used to predict the lifetimes of noble gas bubbles and their coarsening kinetics under thermal annealing at $0.5T_m$. The coarsening behavior of noble gas bubbles via Ostwald ripening mechanism is identified and gas bubbles with large noble gas atoms show stronger coarsening resistance due to the high dissociation energies of gas-vacancy clusters and the low thermal emission rates of gas atoms from bubbles.

Irradiation creates excess point defects in host materials and could lead to the instability of bubbles and voids, which could thus disorder superlattices. The stability of He GBS in Mo has been studied under *in-situ* Kr ion irradiation at 300 °C [25]. The He GBS gradually becomes disordered under irradiation and the order-disorder transformation completes at 2.5 dpa. The disordering of He GBS is associated with a slight increase in He bubble size and a broader distribution of bubble sizes. Phase-field modeling suggests that irradiation-induced inhomogeneous growth and coarsening of voids and bubbles lead to the disordering of gas bubble and void superlattices. In contrast to the low stability of He GBS under irradiation, the Xe-Kr GBS in irradiated U-Mo shows much higher stability under neutron irradiation up to ~ 1000 dpa [27]. The Xe-Kr GBS in neutron-irradiated U-Mo is nearly perfect in terms of bubble size uniformity and spatial arrangement, while He GBS in Mo always show variations in bubble size and spatial misalignment. The stability of perfect and imperfect void superlattices has been studied and compared using a simplified 2D phase-field model [25]. In a perfect void superlattice without void size and spatial variation, voids grow in a homogeneous manner and superlattice configuration remains stable up to a high dose. In an imperfect void superlattice with spatial deviations from a perfect lattice, voids with smaller inter-void spacing coalesce, leading to the disordering of superlattices. In an imperfect void superlattice with a wide distribution of void sizes, inhomogeneous void growth occurs in voids with varying void radius due to the different absorption rate of point defects. The small voids finally disappear due to void coalescence, and the superlattice becomes disordered as a result. Both inhomogeneous growth and coarsening can be responsible for the disordering of imperfect void superlattices under irradiation.

5. Mechanistic modeling

Several mechanisms have been proposed to understand the formation mechanisms of gas bubble and void superlattices. The importance of material anisotropic properties, such as elastic anisotropy and diffusion anisotropy, on the defect superlattice formation has been emphasized. First, elastic anisotropy is discussed. A phase field model that considers both anisotropic elasticity and anisotropic diffusion of vacancies is developed by Yu and Lu[28]. The model incorporates the free energy of mixing, interfacial energy, and elastic strain energy into the driving force of vacancy diffusion, and the simulations suggest that the orientational preference in vacancy diffusion can be induced by elastic anisotropy. However, this model has difficulties in explaining the formation of void superlattices in bcc W, which is elastically isotropic. Also, it cannot explain the formation of GBS occurring in lower temperature regimes, where diffusion of vacancies is limited. Next, the study of anisotropic diffusion of SIAs is presented. The three-stage formation process of superlattices points to the importance of anisotropic diffusion of SIAs. Evans performed rate theory analysis and concluded that two-dimensional diffusion migration of SIAs causes the concentration variations of SIAs on close-packed planes, leading to the formation of two-dimensional planar ordering of voids and then three-dimensional void lattices [29]. The two-dimensional diffusion mechanism has successfully explained the three-stage formation process of void superlattices and predicted the void lattice structure and the ratio of the void lattice constant to the void radius. Gao et al. developed an instability theory for void superlattice formation within a rate theory framework [30,31]. An instability occurs when the uniform vacancy concen-

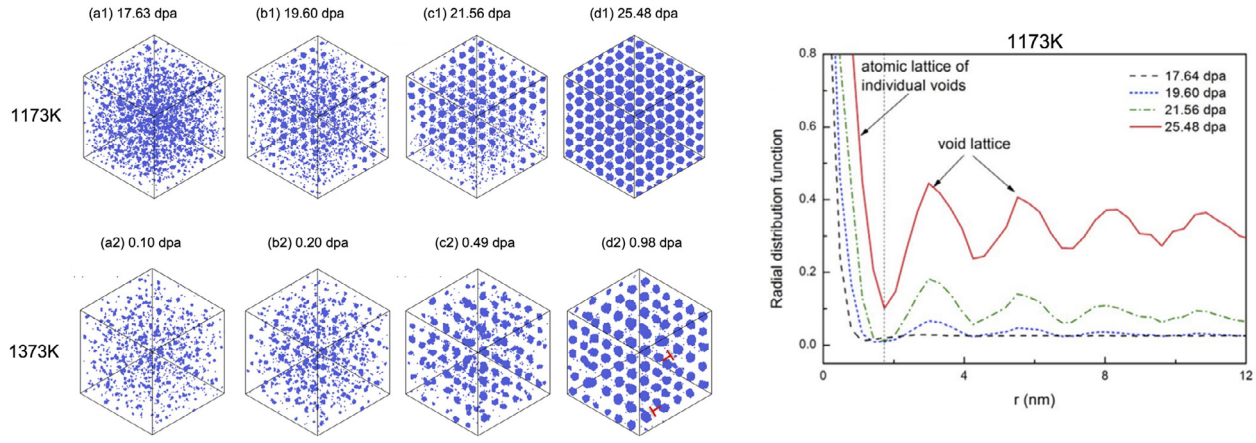

Fig. 4. Snapshots of atomic kinetic Monte Carlo simulations showing the formation process of three-dimensional void lattice in Mo. (a1-d1) at 1173 K, spontaneous phase separation leads to a perfect void superlattice. (a2-d2) at 1373 K, individual void nucleation and growth give less ordering of void lattice. (e) Radial distribution function of vacancies showing nucleation and stabilization of void lattice and evolution of void lattice constant at 1173 K at different dpa levels. [30].

tration field turns into modulated concentration waves. With one-dimensional diffusion of SIAs, symmetrical concentration waves along certain directions will develop, and their superposition leads to a three-dimensional superlattice (Fig. 4). This theory has predicted the irradiation conditions required for void superlattice formation, the dependence of the void superlattice constant on the irradiation conditions (temperature, dose rate, and fluence), and the three-stage formation process of void superlattices. Semenov and Woo considered the effect of isotropic diffusion of vacancies and SIAs that contain a small portion of one-dimensional diffusion of SIAs. Less than 1% one-dimensional diffusion of SIAs leads to the formation of void superlattices [32]. To understand the formation of fcc Xe-Kr GBS in bcc U-Mo, Hu et al. proposed that fast one-dimensional diffusion of U interstitials along <110> directions could lead to the gas bubble alignment along <110> directions in U-Mo [33].

The difference in formation processes between GBS and void superlattices originates from the interaction between gas atoms and host materials. Density-funcational thoery-based *ab initio* calculations are performed to predict lattice site preference, formation energetics, binding energies with vacancies, and migration path and barriers of noble gas atoms (from He to Kr) in bcc transition metals [34]. Although He consistently prefers tetrahedral sites over octahedral sites in all bcc transition metals, Ne, Ar, and Kr prefer octahedral sites in group 5B (V, Nb, and Ta) and tetrahedral sites in group 6B (Cr, Mo, and W) and 8B (Fe) metals. The formation energy of noble gas atoms increases with the atomic size of the gas atoms and with the charge density at the sites where the gas atoms are located. Larger noble gas atoms and higher charge densities lead to more perturbation in the local electron density due to the repulsion between the gas atoms and the charge field. The high formation energy leads to strong binding between gas atoms and vacancies. This can explain the exceptional thermal stability of Xe-Kr GBS compared with He GBS. The presence of gas atom-vacancy complexes effectively suppresses the recombination of vacancies and SIAs and stabilize vacancy clusters. This lowers the temperature required for GBS formation, consistent with the experimental observation that GBS typically form at lower temperatures compared to void superlattices.

6. Summary and outlook

This short review summarizes the recent research progress in the formation, characterization, and modeling of defect superlattices in metals and alloys under irradiation. The development of bubble and void superlattices is strongly linked to the irradiation conditions (temperature, ion fluence, flux, and appm/dpa ratio) and materials properties (chemical complexity and crystal structures). The advance in high-energy X-ray characterization provides more insights into the structure, chemical distribution, and lattice strain of defect superlattices, allowing the development of more comprehensive models for superlattice prediction. Anisotropic materials properties, including elastic anisotropy and diffusion anisotropy, show important implications for defect superlattice formation. Despite the recent research progress of understanding defect superlattices under irradiation, there remain many questions still to be answered.

First, the role of anisotropic diffusion of SIA clusters on the defect superlattice formation remains unclear. The anisotropic diffusion of SIAs can explain the defect ordering in a large number of materials systems; however, it cannot be applied to understand the GBS formation in metals, such as bcc Fe, where SIAs diffuse isotropically. In addition to the anisotropic diffusion of SIAs, one-dimensional diffusion of SIA clusters is also expected to cause the ordering of defects. Small interstitial-type clusters could exhibit higher diffusion anisotropy compared to SIAs. One-dimensional diffusion of interstitial-type loops with Burgers vector of 1/2<111> is reported in α-Fe [35], supporting the SIA cluster diffusion hypothesis. Additional theoretical research is needed to understand the role of anisotropic diffusion of small SIA clusters on the gas bubble and void superlattices.

Second, the mechanisms and kinetics of order-disorder transformation under irradiation are not well understood. The imperfectness of void superlattices could accelerate disordering due to the inhomogeneous growth and coarsening of voids under irradiation. For GBS, the pressurized bubbles could be in gaseous, liquid, or solid state, depending on the atomic radius of gas atoms and irradiation conditions. The disordering mechanism of GBS under irradiation could be different than void superlattices. The critical dose for the order-disorder transformation is dramatically different in different noble gas bubble superlattices (e.g., He GBS at 2.5 dpa, while Xe-Kr GBS at $\sim$ 1000 dpa). The disordering kinetics could also be dependent on irradiation conditions. The influence of irradiation temperature, flux, and gas atom appm/dpa ratio on the disordering kinetics of gas bubble and void superlattices needs further examination.

Lastly, the effect of applied stress on the formation of defect superlattices has not been fully studied. Applied stress shows a considerable impact on the activation energy and migration paths of defects. In bcc Fe, stress could induce anisotropy of migration

rates along different directions and cause the rotation from <111> to <100> of SIAs [36]. The energy landscape between <111> and <110> dumbbells in bcc Mo is very shallow and suggested that very small stresses within the sample would make the <111> dumbbells rotate [37]. As such, the anisotropic diffusion path of SIAs could be altered by the applied stress. Experimentally, the formation of tetragonal He GBS in bulk Mo is attributed to the heterogeneous stress created by bubble swelling, while a full understanding of the effect of stress on the superlattice structures is still missing.

Declaration of Competing Interest

The authors declare that they have no known competing financial interests or personal relationships that could have appeared to influence the work reported in this paper.

CRediT authorship contribution statement

Cheng Sun: Writing – original draft, Writing – review & editing, Funding acquisition.

Acknowledgment

This work is sponsored by the U.S. Department of Energy (DOE) Office of Science, Basic Energy & Science, Materials Sciences and Engineering Division under FWP #C000–14–003 at Idaho National Laboratory, operated by Battelle Energy Alliance under contract DE-AC07–05ID14517. The support from the current and previous project members, Jian Gan, Yongfeng Zhang, Chao Jiang, Andrea M. Jokisaari, Larry K. Aagesen, Anton Schneider, Yipeng Gao, Ericmoore Jossou, Simerjeet K. Gill, Lynne Ecker, and David Sprouster, is gratefully acknowledged. The author also acknowledges Prof. John H. Evans for the discussion and valuable comments.

References

[1] X. Jia, J. Li, E. Wang, Supramolecular self-assembly of morphology-dependent luminescent Ag nanoclusters, Chem. Commun. 50 (2014) 9565–9568, doi:10.1039/c4cc03913k.
[2] M. Tonks, D. Andersson, R. Devanathan, R. Dubourg, A. El-Azab, M. Freyss, F. Iglesias, K. Kulacsy, G. Pastore, S.R. Phillpot, M. Welland, Unit mechanisms of fission gas release: current understanding and future needs, J. Nucl. Mater. 504 (2018) 300–317, doi:10.1016/j.jnucmat.2018.03.016.
[3] J.H. Evans, Observations of a regular void array in high purity molybdenum irradiated with 2 MeV nitrogen ions, Nature 229 (1971) 403–404, doi:10.1038/229403a0.
[4] K. Krishan, Ordering of voids and gas bubbles in radiation environments, Radiat. Eff. 66 (1982) 121–155, doi:10.1080/00337578208222474.
[5] K. Krishan, Void ordering in metals during irradiation, Philos. Mag. A 45 (1982) 401–417, doi:10.1080/01418618208236179.
[6] B.A. Loomis, S.B. Gerber, A. Taylor, Void ordering in ion-irradiated Nb and Nb-1% Zr, J. Nucl. Mater. 68 (1977) 19–31, doi:10.1016/0022-3115(77)90212-4.
[7] J. Bentley, Void shrinkage and void lattice formation in neutron-irradiated molybdenum, Microsc. Microanal. 19 (2013) 1790–1791, doi:10.1017/S1431927613010945.
[8] N.M. Ghoniem, D. Walgraef, S.J. Zinkle, Theory and experiment of nanostructure self-organization in irradiated materials, Journal of Computer-Aided Materials Design 8 (2002) 1–38.
[9] P.B. Johnson, D.J. Mazey, Gas-bubble superlattice formation in bcc metals, J. Nucl. Mater. 218 (1995) 273–288, doi:10.1016/0022-3115(94)00674-1.
[10] C. Sun, D.J. Sprouster, Y. Zhang, D. Chen, Y. Wang, L.E. Ecker, J. Gan, Formation window of gas bubble superlattice in molybdenum under ion implantation, Phys. Rev. Mater. 3 (2019) 103607, doi:10.1103/PhysRevMaterials.3.103607.
[11] D.J. Sprouster, C. Sun, Y. Zhang, S.N. Chodankar, J. Gan, L.E. Ecker, Irradiation-dependent helium gas bubble superlattice in tungsten, Sci. Rep. 9 (2019) 2277, doi:10.1038/s41598-019-39053-0.
[12] R.W. Harrison, G. Greaves, J.A. Hinks, S.E. Donnelly, Engineering self-organising helium bubble lattices in tungsten, Sci. Rep. 7 (2014) 7724, doi:10.1038/s41598-017-07711-w.
[13] R.W. Harrison, G. Greaves, H. Le, H. Bei, Y. Zhang, S.E. Donnelly, Chemical effects on He bubble superlattice formation in high entropy alloys, Curr. Opin. Solid State Mater. Sci. 23 (2019) 100762, doi:10.1016/j.cossms.2019.07.001.
[14] J.H. Evans, A.J.E. Foreman, R.J. McElroy, Anisotropic diffusion of self-interstitials in zirconium, J. Nucl. Mater. 168 (1989) 340–342, doi:10.1016/0022-3115(89)90601-6.
[15] D.J.J. Mazey, J.H.H. Evans, Bubble lattice formation in titanium injected with krypton ions, J. Nucl. Mater. 138 (1986) 16–18, doi:10.1016/0022-3115(86)90248-5.
[16] S.M. Liu, S.H. Li, W.Z. Han, Effect of ordered helium bubbles on deformation and fracture behavior of α-Zr, J. Mater. Sci. Technol. 35 (2019) 1466–1472, doi:10.1016/J.JMST.2019.03.015.
[17] C. Sun, D.J. Sprouster, K. Hattar, L.E. Ecker, L. He, Y. Gao, Y. Zhang, J. Gan, Formation of tetragonal gas bubble superlattice in bulk molybdenum under helium ion implantation, Scr. Mater. 149 (2018) 26–30, doi:10.1016/J.SCRIPTAMAT.2018.01.023.
[18] J. Gan, D.D. Keiser, D.M. Wachs, A.B. Robinson, B.D. Miller, T.R. Allen, Transmission electron microscopy characterization of irradiated U-7Mo/Al-2Si dispersion fuel, J. Nucl. Mater. 396 (2010) 234–239, doi:10.1016/j.jnucmat.2009.11.015.
[19] D.J. Sprouster, R. Giulian, L.L. Araujo, P. Kluth, B. Johannessen, N. Kirby, M.C. Ridgway, Formation and structural characterization of Ni nanoparticles embedded in SiO_2, J. Appl. Phys. 109 (2011) 113517, doi:10.1063/1.3594751.
[20] C. Sun, C. Jiang, E. Jossou, M. Topsakal, S.K. Gill, L.E. Ecker, J. Gan, Self-assembly of solid nanoclusters in molybdenum under gas ion implantation, Scr. Mater. 194 (2021) 113651, doi:10.1016/j.scriptamat.2020.113651.
[21] S.K. Gill, M. Topsakal, E. Jossou, X. Huang, K. Hattar, J. Mausz, M. Elbakhshwan, H. Yan, Y.S. Chu, C. Sun, L. He, J. Gan, L. Ecker, Impact of krypton irradiation on a single crystal tungsten: multi-modal X-ray imaging study, Scr. Mater. 188 (2020) 296–301, doi:10.1016/J.SCRIPTAMAT.2020.07.024.
[22] E. Jossou, A. Schneider, C. Sun, Y. Zhang, S. Chodankar, D. Nykypanchuk, J. Gan, L. Ecker, S.K. Gill, Unraveling the early-stage ordering of krypton solid bubbles in molybdenum: a multimodal study, J. Phys. Chem. C 125 (2021) 23338–23348, doi:10.1021/acs.jpcc.1c05591.
[23] J. Gan, D.D. Keiser, B.D. Miller, A.B. Robinson, D.M. Wachs, M.K. Meyer, Thermal stability of fission gas bubble superlattice in irradiated U-10Mo fuel, J. Nucl. Mater. 464 (2015) 1–5, doi:10.1016/j.jnucmat.2015.04.023.
[24] J. Gan, C. Sun, L. He, Y. Zhang, C. Jiang, Y. Gao, Thermal stability of helium bubble superlattice in Mo under TEM *in-situ* heating, J. Nucl. Mater. 505 (2018) 207–211, doi:10.1016/J.JNUCMAT.2018.04.030.
[25] C. Sun, Y. Gao, D.J. Sprouster, Y. Zhang, D. Chen, Y. Wang, L.E. Ecker, J. Gan, Disordering of helium gas bubble superlattices in molybdenum under ion irradiation and thermal annealing, J. Nucl. Mater. 539 (2020) 152315, doi:10.1016/j.jnucmat.2020.152315.
[26] C. Jiang, Y. Zhang, L.K. Aagesen, A.M. Jokisaari, C. Sun, J. Gan, Noble gas bubbles in bcc metals: ab initio-based theory and kinetic monte carlo modeling, Acta Mater. 213 (2021) 116961, doi:10.1016/J.ACTAMAT.2021.116961.
[27] B.D. Miller, J. Gan, D.D. Keiser, A.B. Robinson, J.F. Jue, J.W. Madden, P.G. Medvedev, Transmission electron microscopy characterization of the fission gas bubble superlattice in irradiated U-7 wt%Mo dispersion fuels, J. Nucl. Mater. 458 (2015) 115–121, doi:10.1016/j.jnucmat.2014.12.012.
[28] H.C. Yu, W. Lu, Dynamics of the self-assembly of nanovoids and nanobubbles in solids, Acta Mater. 53 (2005) 1799–1807, doi:10.1016/j.actamat.2004.12.029.
[29] J.H. Evans, Simulations of the effects of 2-D interstitial diffusion on void lattice formation during irradiation, Philos. Mag. 86 (2006) 173–188, doi:10.1080/14786430500380134.
[30] Y. Gao, Y. Zhang, D. Schwen, C. Jiang, C. Sun, J. Gan, M. Bai, Theoretical prediction and atomic kinetic monte carlo simulations of void superlattice self-organization under irradiation, Sci. Rep. 8 (2018) 6629, doi:10.1038/s41598-018-24754-9.
[31] Y. Gao, Y. Zhang, D. Schwen, C. Jiang, C. Sun, J. Gan, Formation and self-organization of void superlattices under irradiation: a phase field study, Materialia 1 (2018) 78–88, doi:10.1016/j.mtla.2018.04.003.
[32] A.A. Semenov, C.H. Woo, Void lattice formation as a nonequilibrium phase transition, Phys. Rev. B 74 (2006) 24108, doi:10.1103/PhysRevB.74.024108.
[33] S. Hu, D.E. Burkes, C.A. Lavender, D.J. Senor, W. Setyawan, Z. Xu, Formation mechanism of gas bubble superlattice in UMo metal fuels: phase-field modeling investigation, J. Nucl. Mater. 479 (2016) 202–215, doi:10.1016/j.jnucmat.2016.07.012.
[34] C. Jiang, Y. Zhang, Y. Gao, J. Gan, Ab initio theory of noble gas atoms in bcc transition metals, Phys. Chem. Chem. Phys. 20 (2018) 17048–17058, doi:10.1039/C8CP01817K.
[35] K. Arakawa, K. Ono, M. Isshiki, K. Mimura, M. Uchikoshi, H. Mori, Observation of the one-dimensional diffusion of nanometer-sized dislocation loops, Science 80 (2007) 318, doi:10.1126/science.1145386.
[36] Z. Chen, N. Kioussis, N. Ghoniem, D. Seif, Strain-field effects on the formation and migration energies of self interstitials in α-Fe from first principles, Phys. Rev. B 81 (2010) 94102, doi:10.1103/PhysRevB.81.094102.
[37] S. Han, L.A. Zepeda-Ruiz, G.J. Ackland, R. Car, D.J. Srolovitz, Self-interstitials in V and Mo, Phys. Rev. B 66 (2002) 220101, doi:10.1103/PhysRevB.66.220101.